Fluorescence-Based Evaluation of the Partitioning of Lipids and Lipidated Peptides into Liquid-Ordered Lipid Microdomains: A Model for Molecular Partitioning into "Lipid Rafts"

Tian-Yun Wang, Rania Leventis, and John R. Silvius
Department of Biochemistry, McGill University, Montréal, Québec H3G 1Y6, Canada

ABSTRACT A fluorescence-quenching assay is described that can directly monitor the relative extents of partitioning of different but structurally homologous fluorescent molecules into liquid-ordered (l_o) domains in lipid vesicles exhibiting liquid-ordered/liquid-disordered (l_o/l_d) phase coexistence. Applying this assay to a series of bimane-labeled diacyl phospholipid probes in cholesterol-containing ternary lipid mixtures exhibiting l_o/l_d phase separation, we demonstrate that partitioning into l_o-phase domains is negligible for diunsaturated species and greatest for long-chain disaturated species. These conclusions agree well with those derived from previous studies of the association of lipids and lipid-anchored molecules with l_o-phase domains, using methods based on the isolation of a detergent-insoluble fraction from model or biological membranes at low temperatures. However, we also find that monounsaturated and shorter-chain saturated species partition into l_o phases with significant, albeit modest affinities, and that the level of partitioning of these latter species into l_o-phase domains is significantly underestimated (relative to that of their long-chain saturated counterparts) by the criterion of low-temperature detergent insolubility. Finally, applying the fluorescence-quenching method to a family of lipid-modified peptides, we demonstrate that the *S*-palmitoyl/*S*-isoprenyl dual-lipidation motif found in proteins such as H- and N-ras and yeast Ste18p does not promote significant association with l_o domains in l_o/l_d-phase-separated bilayers.

INTRODUCTION

Accumulating evidence in recent years has suggested that the lipids of the plasma and certain other membranes of animal cells do not comprise a homogeneous fluid bilayer but instead may form laterally segregated domains with distinct lipid compositions and physical properties (for recent reviews see Brown, 1998; Brown and London, 1997, 1998a, 1998b; Rietveld and Simons, 1998; Simons and Ikonen, 1997). Early findings that a fraction of the membrane lipids of mammalian cells were resistant to solubilization by certain nonionic detergents at low temperatures (Brown and Rose, 1992; Cinek and Horejsí, 1992; Sargiacomo et al., 1993) and supportive data reported subsequently for lipid model systems (Ahmed et al., 1997; Schroeder et al., 1994, 1998) have suggested that a fraction of the lipids in cholesterol-containing membranes may exist in liquid-ordered (l_o) domains that coexist with lipid-disordered (l_d) regions within the membrane bilayer. Intriguingly, the low-density membrane remnants isolated from cell membranes after low-temperature detergent extraction are found to be depleted in most integral membrane proteins but enriched not only in cholesterol and sphingolipids, but also in certain classes of lipidated proteins, notably glycosylphosphatidylinositol-anchored and doubly acylated species (Arni et al., 1998; Brown and Rose, 1992; Cinek and Horejsí, 1992; Melkonian et al., 1999; Rodgers et al., 1994; Sargiacomo et al., 1993; Shenoy-Scaria et al., 1992, 1993; van't Hof and Resh, 1997). It has been suggested that the presence of multiple long saturated acyl chains in these membrane-anchoring motifs favors their association with the l_o-phase and consequently with "lipid raft" structures that are isolated as a low-density, unsolubilized fraction after low-temperature detergent treatment.

To date the distribution of various membrane components between liquid-ordered and liquid-disordered domains in membranes has been inferred largely from the distribution of such molecules between the soluble and insoluble fractions obtained upon low-temperature detergent treatment of biological or model membranes. Recent reports (Ahmed et al., 1997; Silvius, 1992; Silvius et al., 1996) have shown that fluorescence-quenching methods can be employed to monitor l_o/l_d lateral phase separations in ternary (lipid/lipid/sterol) systems. We have here adapted such measurements to compare the distribution of various fluorescent-labeled lipids and lipidated peptides between l_o and l_d domains in representative mixtures combining saturated sphingo- or phospholipids with spin-labeled phospholipids and physiological proportions of cholesterol. Our results support previous general conclusions that increasing acyl chain length enhances, while chain unsaturation diminishes, affinity for the l_o phase in bilayers where l_o and l_d phases coexist. However, our data provide a more "nuanced" picture of this relationship than do procedures based on low-temperature detergent fractionation, notably demonstrating that in addition to long-chain saturated species, monounsaturated and shorter-chain saturated species may also exhibit significant, if weaker, affinities for the l_o phase under these conditions. Finally, using the same methodology, we demonstrate that

Received for publication 22 February 2000 and in final form 20 April 2000.

Address reprint requests to Dr. John R. Silvius, Department of Biochemistry, McGill University, Room 8-19, McIntyre Building, 3655 rue Drummond, Montréal, Québec H3G 1Y6, Canada. Tel.: 514-398-7267; Fax: 514-398-7384; E-mail: silvius@med.mcgill.ca.

© 2000 by the Biophysical Society

0006-3495/00/08/919/15 $2.00

prenylated peptides show little affinity for l_o-phase domains, even when the peptides are additionally modified with an *S*-palmitoyl residue.

MATERIALS AND METHODS

Materials

Bimane-labeled lipidated peptides were synthesized and purified by methods described previously (Shahinian and Silvius, 1995; Silvius and l'Heureux, 1994). 1,2-Dioleoylphosphatidyl-*N*,*N*-dimethyl-*N*-(2,2,6,6-tetramethyl-4-piperidinyl)-ethanolamine (TEMPO-DOPC) and TEMPO-choline were synthesized as described previously (Gaffney, 1976). *N*-(Bimanylthioacetyl)-labeled diacyl phosphatidylethanolamines (BimtaPEs) were synthesized as follows. The succinimidyl ester of *S*-bimanylmercaptoacetic acid was first prepared by reacting together 1.0, 1.1, and 1.5 equivalents of *S*-bimanylmercaptoacetic acid (Schroeder et al., 1997), dicyclohexylcarbodiimide, and *N*-hydroxysuccinimide for 4 h in 1:1 (v/v) dry CH_2Cl_2/dimethylformamide (0.05 M in *S*-bimanylmercaptoacetic acid). After it was filtered through a small glass wool plug, the solution was combined with 0.7 eq (based on bimanylmercaptoacetic acid) of diacyl PE and 1 eq of diisopropylethylamine in 3:1 CH_2Cl_2 (10 mM in PE), then incubated overnight. After partitioning the products between CH_2Cl_2 and 1:1 methanol/0.1 M aq. HCOONa (pH 3.0), the lower phase was recovered and dried down, first under a stream of nitrogen and then under high vacuum for several hours. The labeled PE was finally purified by preparative thin-layer chromatography (TLC) in 80:20:1 (v/v/v) CH_2Cl_2/methanol/conc. NH_4OH. (*S*-Bimanylmercaptosuccinyl)-bisPEs (BMS-bisPEs) (structure shown in Fig. 1) were synthesized by reacting 1 eq of an (*S*-bimanylmercaptosuccinyl)-PE (Silvius and Zuckermann, 1993) with 2 eq of the appropriate diacyl PE in 2:1:0.5 (v/v/v) methanol/chloroform/0.1 M aq. potassium phosphate (pH 8.0) at 45°C, using 1-ethyl-2-(3-dimethylaminopropyl)carbodiimide (4 eq) as the condensing agent, and were purified by preparative TLC. Bovine brain sphingomyelin and cerebroside were obtained from Avanti Polar Lipids (Alabaster, AL); synthetic phospholipids were obtained from this source or from Sigma (St. Louis, MO). Common chemicals were obtained from Sigma or Fisher Scientific (Ville-St.-Laurent, Québec).

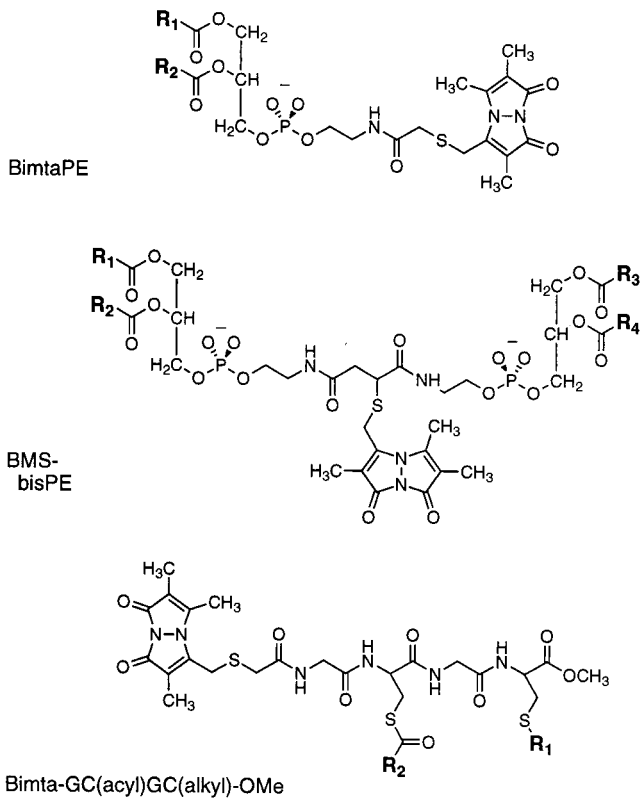

FIGURE 1 General structures of the lipid probes used in this study.

Vesicle preparation and fluorescence assays

Lipid mixtures (normally 75 nmol total lipid, including 0.6 mol% of a fluorescent lipid or lipidated peptide) were mixed as stock solutions in methylene chloride/methanol (3:1) then dried down under nitrogen while being warmed to 50–55°C. Samples containing lipidated peptides were subsequently redissolved in 9:1 (v/v) cyclohexane/ethanol with brief heating to 80°C, rapidly frozen in dry ice/ethanol, and lyophilized. After initial drying under nitrogen as described above, samples containing fluorescent lipids were either lyophilized in the same manner or in some cases simply incubated for 6–12 h under high vacuum when it was first established that the two methods gave equivalent results.

Dried or lyophilized samples were rehydrated in 1 ml of 100 mM NaCl, 0.1 mM EDTA, 10 mM 3-(*N*-morpholino)propanesulfonic acid (MOPS) (pH 7.2) (for samples containing lipid probes) or 100 mM NaCl, 0.1 mM EDTA, 10 mM sodium phosphate (pH 5.0) (for samples containing lipidated peptides); use of the latter buffer avoided hydrolysis of *S*-acylated lipopeptides during subsequent sample incubations. Fluorescent lipid-containing samples were incubated for 15 min at 45°C, warmed to 65°C for 1 min (or to 85°C for 1 min for sphingolipid-containing samples), vortexed for 10 s, incubated for a further 10 min at 45°C, then gradually cooled (at ~0.3°C/min) to the final experimental temperature and finally incubated at this latter temperature for 1–6 h (using longer incubations for lower incubation temperatures). Lipidated peptide-containing samples were prepared similarly, except that the period of incubation at 65°C was shortened to 20 s, again to avoid hydrolysis of *S*-acyl groups. Control experiments showed that the quenching curves measured subsequently were not significantly altered when sample incubations at the final experimental temperature were prolonged to 6–12 h, or when hydrated samples were cooled 10°C below the desired final incubation temperature, incubated for 30 min at the lower temperature, and then further incubated at the experimental temperature as described above. Sample fluorescence was finally determined with a Perkin-Elmer LS-5 spectrofluorometer ($\lambda_{ex}/\lambda_{em}$ = 390 nm/468 nm), first after the samples were diluted to 3 ml in buffer and again after 1% (w/v) Triton X-100 was added and the samples were heated for 15 min to 45°C and for 1 min to 65°C (or 75°C for sphingolipid-containing samples), bath-sonicated for 10 s, and finally reincubated at 45°C for 15 min. These data and appropriate blank readings were used to calculate the normalized fluorescence values F_N, defined as the ratio of the (blank-corrected) fluorescence of a sample to the (blank-corrected) fluorescence measured after subsequent solubilization in Triton X-100 as just described. Fluorescence-quenching results presented here represent the averages of data obtained in two to four independent experiments.

Analysis of fluorescence-quenching data

The experimental quenching curves measured for different homologous fluorescent species in the same ternary lipid system at the same temperature, plotted in the scaled form $(F/F_o)_{cor}$ given by Eq. 3 in the Theory

section, were fitted on an empirical basis to the following equation:

$$(F/F_o)_{cor} = (F/F_o)^{max}_{cor} \cdot K \cdot \left(\frac{x^{ld}_Q - x_Q}{(x_Q - x^{lo}_Q) + K \cdot (x^{ld}_Q - x_Q)} \right) + (F/F_o)^{min}_{cor} \cdot \left(\frac{x_Q - x^{lo}_Q}{(x_Q - x^{lo}_Q) + K \cdot (x^{ld}_Q - x_Q)} \right) \quad (1)$$

where x_Q represents the mole fraction of spin-labeled (quencher) phosphatidylcholine in the nonsterol fraction, x^{lo}_Q and x^{ld}_Q are the values of x_Q defining the l_o-phase-only and the l_d-phase-only boundaries of the region of phase separation (at 33 mol% cholesterol), and K, $(F/F_o)^{max}_{cor}$, and $(F/F_o)^{min}_{cor}$ are empirical fitting parameters (for the application of this equation to binary systems see London and Feigenson, 1981). Values of x^{lo}_Q and x^{ld}_Q were first estimated by inspection of the complete set of quenching curves for the different homologous fluorescent probes, then the different quenching curves were fit independently to Eq. 1, with K, $(F/F_o)^{max}_{cor}$, and $(F/F_o)^{min}_{cor}$ as adjustable parameters. The points of intersection of the various fitted curves were then determined, and the center of mass of the cluster of intersection points was calculated to provide a refined "consensus" estimate of x^{ld}_Q and $(F/F_o)^{min}_{cor}$. Using these latter values and the original estimate of x^{lo}_Q, we refitted the quenching curves for the various homologous fluorescent species to Eq. 1, with K and $(F/F_o)^{max}_{cor}$ as adjustable parameters. The slopes of the final fitted curves at $x_Q = x^{ld}_Q$ were then calculated as

$$\left. \frac{d(F/F_o)_{cor}}{dx_Q} \right|_{x_Q = x^{ld}_Q} = -\left(\frac{K \cdot ((F/F_o)^{max}_{cor} - (F/F_o)^{min}_{cor})}{(x^{ld}_Q - x^{lo}_Q)} \right) \quad (2)$$

and scaled as discussed in the Results (Eq. 8) to give the values presented in Table 1. The results compiled in Table 1 were found to be essentially invariant with reasonable variations in the choice of the parameter x^{lo}_Q. The standard errors of the estimated slope values and of the derived values presented were estimated using standard propagation-of-error analyses (Barrantes, 1998).

Detergent-solubilization assays

Lipid solubilization assays were carried out using the method of Schroeder et al. (1994), with minor modifications. Unilamellar lipid vesicles, composed of 1:1:1 dipalmitoylphosphatidylcholine/1-palmitoyl-2-(12-doxylstearoyl)-phosphatidylcholine/cholesterol (DPPC/12SLPC/cholesterol) or bovine brain sphingomyelin/12SLPC/cholesterol and labeled with 0.6 mol% BimtaPE, were prepared by extrusion of hydrated lipid samples, prepared as described above, through 0.1-μm pore size polycarbonate filters (MacDonald et al., 1991). All subsequent fractionation steps were carried out at 0–4°C. Vesicle samples (250 nmol lipid) were incubated for 30 min in 3.5 ml of buffer (100 mM NaCl, 10 mM MOPS, 0.1 mM EDTA, pH 7.2) containing 1% (v/v) Triton X-100, then centrifuged at 200,000 × *g* for 2 h. The upper 3 ml of supernatant was carefully removed and retained, the residual supernatant was carefully removed separately, and the pellet and lower supernatant fractions were finally diluted to 3 ml in Triton-containing buffer. The recovered pellet and supernatant fractions were then warmed to 65°C for 1 min, incubated at 45°C for 5 min, bath-sonicated for 15 s, and further incubated at 45°C for 30 min before we read the BimtaPE fluorescence in each fraction at 25°C as described above. The appropriately blank-corrected fluorescence readings were used to calculate the proportions of each BimtaPE recovered in the pellet and supernatant fractions.

THEORY

The systems examined in this study incorporated small amounts of fluorescent lipids or lipidated peptides into lipid vesicles combining a constant proportion of cholesterol (33 mol%), a spin-labeled phosphatidylcholine, which quenches the probe fluorescence, and unlabeled phospho- or sphingolipids. Quenching curves were determined for different fluorescent probes by measuring their fluorescence as a function of the relative proportions of spin-labeled versus unlabeled phospho- or sphingolipids in the vesicles (see, for example, Fig. 2). For simplicity, quenching curves are plotted as a function of the molar percentage of spin-labeled quencher lipid (%Q) in the nonsterol lipid fraction (i.e., the total phospho- plus sphingolipid fraction). (For the systems examined here, containing 33 mol% cholesterol, the molar percentage of the spin-labeled PC in the nonsterol fraction is equal to (100%/0.67) times the mole fraction of this species in the total lipid fraction (including cholesterol).) The *y* axis of the quenching curve for a given fluorescent species X is plotted either as the normalized fluorescence, measured as discussed in Materials and Methods, or, as suggested by London and co-workers (Ahmed et al., 1997; Chattopadhyay and London, 1987), in the alternative scaled form $(F/F_o)_{cor}$:

$$(F/F_o)_{cor} = (F_N - F_{100\%Q})/(F_{0\%Q} - F_{100\%Q}) \quad (3)$$

where F_N is the normalized fluorescence measured for the probe in vesicles of a given composition and $F_{100\%Q}$ and $F_{0\%Q}$ are the normalized fluorescence values measured in vesicles containing, respectively, 100% or 0% quencher lipid in the nonsterol fraction.

When the lipid components form a single phase over the full range of bilayer compositions examined, quenching curves can be well fit by the general equation suggested by London and Feigenson (1981):

$$(F/F_o)_{cor} = A \cdot \exp(-K \cdot (\%Q)) + B \quad (4)$$

where A and B are scaling constants and K is a function of the critical distance for quenching of probe fluorescence by the spin-labeled species; an expression of similar form describes the variation of F_N with (%Q). If, in contrast, the system exhibits a liquid-ordered/liquid-disordered (l_o/l_d) phase separation over part of the range of compositions spanned by the quenching curve, within the region of phase separation the quenching curve will deviate from the form of Eq. 4 and instead will exhibit the alternative form,

$$(F/F_o)_{cor}(X) = f_{ld}(X) \cdot (F/F_o)^{ld}_{cor}(X) + f_{lo}(X) \cdot (F/F_o)^{lo}_{cor}(X) \quad (5)$$

where $(F/F_o)^{ld}_{cor}(X)$ and $(F/F_o)^{lo}_{cor}(X)$ represent the scaled fluorescence values, and $f_{ld}(X)$ and $f_{lo}(X)$ represent the fractions ($f_{ld}(X) + f_{lo}(X) = 1$) of the probe X in the coexisting l_d and l_o phases, respectively. This equation is quite general and can be applied (with appropriate changes of subscripts) to other types of lipid lateral phase separations as well.

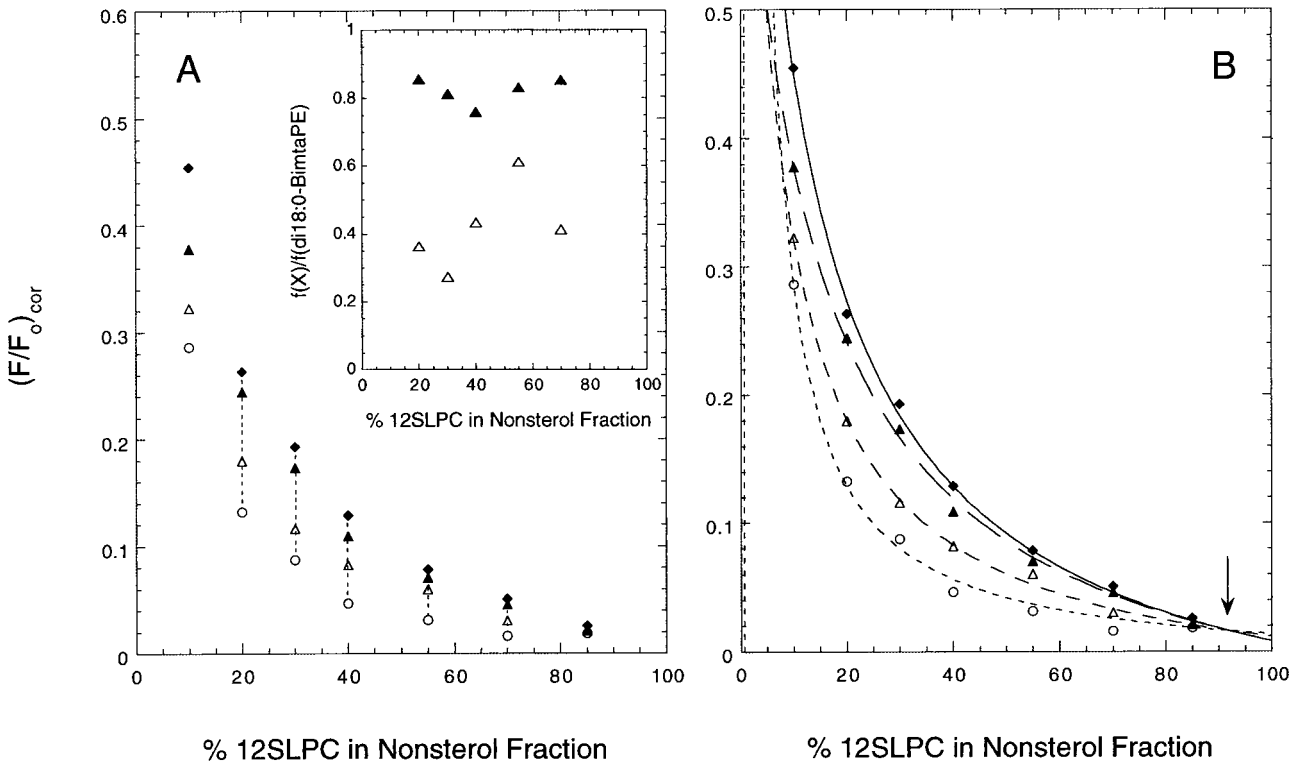

FIGURE 2 Illustrative analyses of quenching curves to determine the relative extent of partitioning of different BimtaPEs into the l_o phase (f_{lo}) compared to that of di18:0-BimtaPE. As noted in the text, the bilayer content of spin-labeled (quencher) PC is indicated on the *x* axis as the molar percentage of this species in the nonsterol fraction (i.e., in the total phospho- plus sphingolipid fraction), which thus can range from 0 to 100 mol%. Details of sample preparation and data collection were as described in Materials and Methods. (*A*) Scaled fluorescence data obtained for di18:0- (◆), di16:0- (▲), 18:0/18:1c- (△), and di14:1c-BimtaPEs (○) in brain sphingomyelin/12SLPC/(33 mol% cholesterol) bilayers at 37°C. At each composition analyzed (data lying along *dashed lines* in main figure), the ratio $f_{lo}(X)/f_{lo}(di18:0)$ (*inset*) was estimated for di16:0- (▲) and 18:0/18:1c-BimtaPE (△), using Eq. 7 to give the values shown in the inset. (*B*) Quenching curves for the same BimtaPEs (symbols as in *A*) were fit to Eq. 1, with a common point of intersection (*arrow*) defining the estimated right-hand boundary of the region of phase separation ($x_Q = x_Q^{ld}$) as described in the text. The slopes of the fitted curves at this boundary were then used to estimate the value of $f_{lo}(X)/f_{lo}(di18:0)$ for each BimtaPE according to Eq. 8, giving the values indicated in Table 1. The fitted curves shown were determined using the common intersection point estimated from the data obtained for all of the BimtaPEs examined in this system (Fig. 3).

For binary mixtures exhibiting phase separation, Eq. 5 can be converted to Eq. 1 in Materials and Methods, to which quenching data can be fit to determine directly the partition coefficient (K_p) describing the relative affinity of a fluorescent probe for two coexisting lipid phases (Ahmed et al., 1997; London and Feigenson, 1981). Quenching curves for ternary or higher-order systems unfortunately cannot be analyzed in the same direct manner. However, as outlined below, for these more complex systems it is still possible to obtain useful information about the relative affinities of different but related fluorescent species for the l_o phase. Consider a family of homologous bilayer-associated fluorescent probes, all of which carry a common fluorescent label and which vary in structure only in a region of the molecule that is well removed from the fluorescent moiety. (For brevity we here use the term "homologous" to denote species that share a common polar "backbone" structure, fluorescent group, and site of fluorophore attachment but carry different hydrocarbon chains.) Because of their close structural similarity, the different homologous fluorescent species may be expected to exhibit comparable efficiencies of fluorescence quenching in any single phase of a given composition. In this case the value of $(F/F_o)^{ld}_{cor}(X)$ in Eq. 5 will be the same for all homologous species X and likewise for $(F/F_o)^{lo}_{cor}(X)$, so that from Eq. 5 we can derive the expression

$$f_{lo}(X) = \frac{((F/F_o)_{cor}(X) - (F/F_o)^{ld}_{cor})}{((F/F_o)^{lo}_{cor} - (F/F_o)^{ld}_{cor})} \quad (6)$$

where at any given system composition the values of $(F/F_o)^{ld}_{cor}$ and $(F/F_o)^{lo}_{cor}$ are now common to all homologous species.

For ternary and higher-order systems like those examined here, the values of $(F/F_o)^{ld}_{cor}$ and $(F/F_o)^{lo}_{cor}$ in Eqs. 5 and 6, which may vary with the overall composition of the system, cannot be determined from curve fitting or control experiments without very detailed knowledge of the relevant

phase diagrams. Nonetheless, in many cases it may be possible to estimate accurately the value of $(F/F_o)^{ld}_{cor}$, though typically not that of $(F/F_o)^{lo}_{cor}$, as a function of bilayer composition. In such cases, while we cannot use Eq. 6 to determine the absolute fraction of any given probe that is partitioned into the l_o phase in a given phase-separated lipid mixture, we can nonetheless determine the relative extents of partitioning of two different homologous species X and Y into the l_o phase, using the equation

$$\frac{f_{lo}(X)}{f_{lo}(Y)} = \frac{((F/F_o)_{cor}(X) - (F/F_o)^{ld}_{cor})}{((F/F_o)_{cor}(Y) - (F/F_o)^{ld}_{cor})} \quad (7)$$

In practice the requisite value of $(F/F_o)^{ld}_{cor}$ in Eq. 7 can be determined by using a third member of the same homologous series of probe molecules that exhibits negligible partitioning into the l_o phase, such that for this species $(F/F_o)_{cor} = (F/F_o)^{ld}_{cor}$ at each lipid composition examined.

Quenching curves were analyzed quantitatively by two alternative approaches to determine the relative affinities of fluorescent species for l_o-phase domains in the systems examined here. In Fig. 2 we illustrate the application of these approaches to data obtained for four bimane-labeled phospholipids (BimtaPEs) in the sphingomyelin/12SLPC/(33 mol% cholesterol) system at 37°C, which exhibits an (l_o/l_d) phase separation for compositions ranging from <10 mol% to 80–85 mol% 12SLPC in the nonsterol fraction.

In the first method of quenching-curve analysis, illustrated in Fig. 2 *A*, Eq. 7 is applied directly to data obtained for different probes X at each bilayer composition within the region of phase separation. For the analysis shown di18:0-BimtaPE was designated as the reference species Y, and as discussed in the Results, quenching data for di14:1c-BimtaPE were used to estimate the parameter $(F/F_o)^{ld}_{cor}$. As the open triangles in Fig. 2 *A* (*inset*) illustrate, the resulting ratios $(f_{lo}(X)/f_{lo}(\text{di18:0-BimtaPE}))$, while straightforward to calculate, tend to magnify even modest scatter in the quenching curves where these lie close together, notably for compositions near the right-hand boundary of the region of phase separation. Moreover, near the left-hand boundary of the phase-separation region, the quenching curves for different fluorescent species X also converge as the fraction of l_o-phase lipid approaches unity, suppressing intrinsic differences in the relative affinities of the different homologous probes for the l_o phase.

To address the limitations just noted to the "ratio" analysis illustrated in Fig. 2 *A*, we devised an alternative analysis based on comparisons of the slopes of the quenching curves for different probes at the right-hand (l_d-phase-rich) limit of the region of phase separation. As illustrated in Fig. 2 *B*, within the phase separation region the quenching curves for various homologous BimtaPEs were well described by a hyperbolic function (Eq. 1 in Materials and Methods), which is rigorously applicable only to binary lipid mixtures, but which was used on a purely empirical basis for the more complex systems investigated here. As described in Materials and Methods, the quenching curves obtained for a set of homologous BimtaPEs were fitted simultaneously to pass through a common intersection point (Fig. 2 *B*, *arrow*) defining the right-hand boundary of the region of (l_o/l_d) phase separation. Once again, the data set analyzed included the quenching curve for a homologous species exhibiting negligible partitioning into the l_o phase (di14:1c-BimtaPE). From the calculated slope of the fitted quenching curve for each species at the right-hand boundary of the phase-separation region ($(\text{Slope(X)})|_{x_Q = x_Q^{ld}}$, etc.) we determined the relative extent of partitioning of different species X and Y into the l_o phase from the equation

$$\frac{f_{lo}(X)}{f_{lo}(Y)} = \frac{(\text{Slope(X)})|_{x_Q = x_Q^{ld}} - (\text{Slope}(f_{ld} = 1))|_{x_Q = x_Q^{ld}}}{(\text{Slope(Y)})|_{x_Q = x_Q^{ld}} - (\text{Slope}(f_{ld} = 1))|_{x_Q = x_Q^{ld}}} \quad (8)$$

where $(\text{Slope}(f_{ld} = 1))|_{x_Q = x_Q^{ld}}$ is the analogous slope estimate determined for a species partitioning entirely into the l_d phase (here, di-14:1c-BimtaPE). Because the ratio $(f_{lo}(X)/f_{lo}(Y))$ in Eq. 8 is evaluated at the right-hand extremum of the region of phase separation, where only small amounts of l_o-phase domains are present, this value can be taken to represent the ratio of the (l_o/l_d) phase partition coefficients for species X and Y, at least near the right-hand limit of the region of phase separation. The "slope" analysis does not assess directly whether the relative affinities of different Bimta-PEs for the l_o phase in a given ternary system (compared to that of the reference di18:0 species) may vary with the composition of the system. Our analyses by the "ratio" method of the relative extents of partitioning of different Bimta-PEs into the l_o phase, however, do not provide evidence for large systematic effects of this nature.

RESULTS

Fluorescence quenching of bimane-labeled lipids in homogeneous and (l_o/l_d) phase-separated bilayers

The distribution of a fluorescent molecule between two coexisting phases in lipid bilayers, including cholesterol-containing systems (Ahmed et al., 1997; Silvius, 1992; Silvius et al., 1996), can be monitored by fluorescence measurements if the bilayers include a fluorescence quencher that is unequally distributed between the two phases. In the present study we applied this approach to compare the distributions of different fluorescent-labeled diacylphospholipids and lipidated peptides in ternary mixtures combining a liquid-ordered (l_o) phase-preferring phospho- or sphingolipid; a liquid-disordered (l_d) phase-preferring spin-labeled phospholipid, which acts as a fluorescence quencher; and a fixed proportion (33 mol%) of cholesterol. As discussed in the previous section, by comparing fluorescence-quenching data obtained in such systems for families

of closely related fluorescent molecules, it is possible to determine the relative affinities of the different fluorescent species for the l_o versus the l_d phase.

In Fig. 3 *A* we show quenching curves measured for two bimane-labeled phosphatidylethanolamines (BimtaPEs), with the general structure shown in Fig. 1, in ternary mixtures of DOPC, the spin-labeled quencher lipid 12SLPC, and 33 mol% cholesterol. Bimane-labeled fluorescent molecules were chosen for the experiments described here because the bimane group is uncharged and relatively small and does not itself appear to bind strongly to the membrane polar/apolar interface (Shahinian and Silvius, 1995; Silvius and l'Heureux, 1994; Silvius and Leventis, 1993). In the DOPC/12SLPC/(33 mol% cholesterol) system, which exhibits homogeneous intermixing of the lipid components, BimtaPEs with different acyl chains give essentially identical quenching curves, as illustrated for di18:0- and di-18:1c-BimtaPE in Fig. 3 *A*. As shown in this figure, the quenching curves for the bimane-labeled lipids can be fit well by an exponential expression (Eq. 4) proposed to describe fluorescence quenching by spin-labeled lipids in homogeneous bilayers (London and Feigenson, 1981).

In contrast to the essentially identical quenching curves observed for di18:0- and di18:1c-BimtaPE in the homogeneous system just described, the two lipid probes give markedly divergent quenching curves in the system sphingomyelin/12SLPC/(33 mol% cholesterol), as shown in Fig. 3 *B*. Ahmed et al. (1997) have previously shown that at 37°C the latter system exhibits l_o/l_d phase separation, with the sphingomyelin component enriched in the l_o phase and the 12SLPC component in the l_d phase, over a wide range of relative proportions of sphingomyelin versus 12SLPC (from $<$20 mol% to 80–85 mol% 12SLPC in the nonsterol fraction). Within the region of phase separation the fluorescence of the di18:0 species is seen to be markedly less strongly quenched than that of the di18:1c species, regardless of whether the fluorescence data are plotted as the normalized fluorescence F_N (Fig. 3 *B*, *inset*) or in the scaled form $(F/F_o)_{cor}$ discussed in the previous section (Eq. 3). The divergence of the quenching curves for the two fluorescent lipids within the region of (l_o/l_d) phase separation appears to reflect a difference in the lateral distributions of these species within the phase-separated bilayers, with the di18:0 species partitioning to a significantly greater extent into the quencher-depleted l_o phase.

In Fig. 4 we show fluorescence quenching curves determined for several different diacyl BimtaPE probes in the sphingomyelin/12SLPC/(33 mol% cholesterol) system at

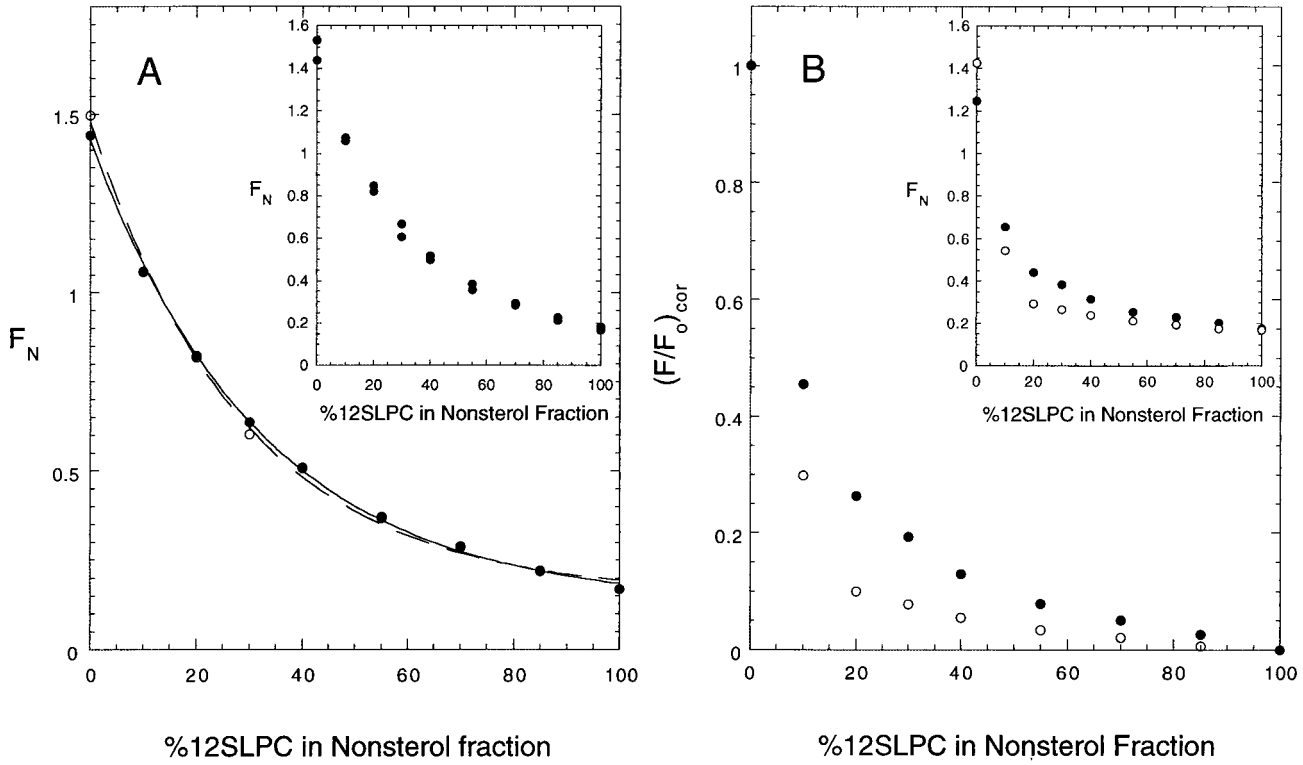

FIGURE 3 (*A*) Quenching curves measured at 37°C for di18:0- (●) and di18:1c-BimtaPE (○) in DOPC/12SLPC/(33 mol% cholesterol) bilayers containing the indicated percentages of 12SLPC in the nonsterol (total phospholipid) fraction. *Inset*: Data obtained for di18:0-BimtaPE in this system in two representative independent experiments. (*B*) Quenching curves obtained at 37°C for di18:0- (●) and di18:1c-BimtaPE (○) in brain sphingomyelin/12SLPC/(33 mol% cholesterol) bilayers containing the indicated percentages of 12SLPC in the nonsterol (total phospholipid plus sphingomyelin) fraction. *Inset*: Same data plotted as normalized fluorescence (F_N) rather than as scaled fluorescence $(F/F_o)_{cor}$, as defined by Eq. 3.

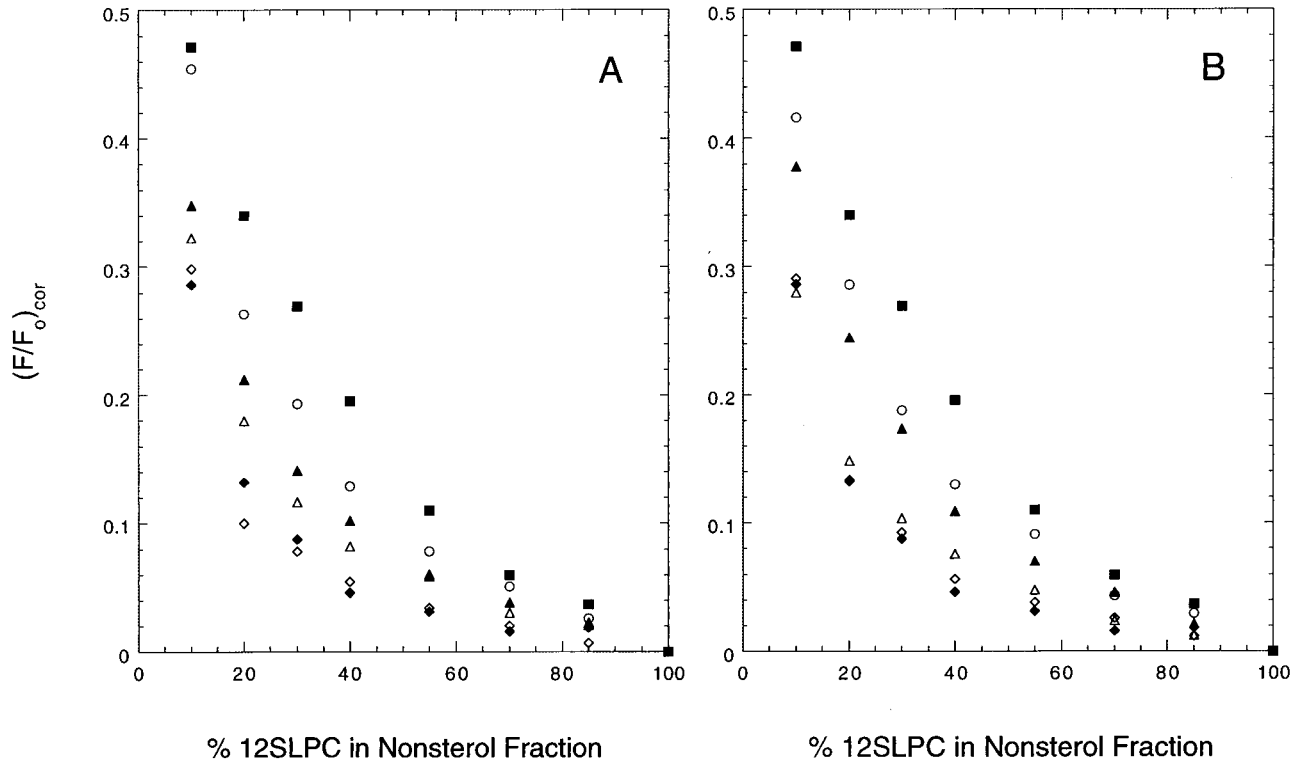

FIGURE 4 Quenching curves obtained at 37°C for bimane-labeled lipids in brain sphingomyelin/12SLPC/(33 mol% cholesterol) bilayers containing the indicated percentages of 12SLPC in the nonsterol (total phospholipid plus sphingomyelin) fraction. (*A*) Quenching data for tetra18:0-BMS-bisPE (■) and for di18:0- (○), di14:0- (▲), 18:0/18:1c- (△), di18:1c- (◇), and di14:1c-BimtaPE (◆). (*B*) Quenching curves determined for tetra18:0- (■) and tetra18:1c-BMS-bisPE (◇) and for di20:0- (○), di16:0- (▲), 16:0/18:1c- (△), and di-14:1cBimtaPE (◆).

37°C. It can be seen that for any given composition within the region of phase separation, the efficiency of fluorescence quenching is greatest for the diunsaturated (di14:1c, di18:1c) species, somewhat less for the monounsaturated (16:0/18:1c, 18:0/18:1c) species, and least for the disaturated species, decreasing as the chain length of the latter species increases. This order of relative quenching efficiencies is preserved over a wide range of relative proportions of sphingomyelin versus 12SLPC.

As discussed in the preceding section, sets of quenching curves like those shown in Fig. 4 can be analyzed quantitatively to determine the relative extents of partitioning of different probes into l_o-phase domains in (l_o/l_d) phase-separated bilayers. To permit such an analysis, two conditions must be fulfilled. First, the different homologous fluorescent species examined must exhibit comparable efficiencies of fluorescence quenching in any single phase of a given composition. For the BimtaPEs examined here this appears to be the case, as attested by the observation that different homologous species exhibit essentially identical quenching curves in the homogeneous DOPC/12SLPC/(33 mol% cholesterol) system described above (Fig. 3 *A*) and in homogeneous DOPC/TEMPO-DOPC/(33 mol% cholesterol) mixtures as well (not shown). An alternative assumption would be that in any single phase of a given composition, all homologous probes exhibit the same normalized fluorescence F_N. We consider this assumption to be less realistic, as while all BimtaPEs examined here gave identical values of F_N in 12SLPC/cholesterol, DOPC/cholesterol, and TEMPO-DOPC/cholesterol mixtures, long-chain disaturated species gave modestly but significantly lower normalized fluorescence values than did other BimtaPEs in sphingolipid/cholesterol and DPPC/cholesterol mixtures, as illustrated in Fig. 2 *B* (*inset*). We nonetheless determined that an analysis based on this alternative assumption would change none of the qualitative conclusions presented here, but that in this case we would estimate that the extents of partitioning of di14:0 and monounsaturated BimtaPEs into l_o domains in mixed-phase bilayers could be up to 35% larger, relative to the partitioning of long-chain saturated BimtaPEs into such domains, than we estimate using the analysis discussed in the text.

Second, at least one of the homologous fluorescent species examined must partition essentially completely into the l_d phase, so that its quenching curve provides information specifically about the fluorescence properties of probe molecules present in this phase ($(F/F_o)^{ld}_{cor}$ in Eq. 7 and (Slope-($f_{ld} = 1$))$|_{x_Q = x_Q^{ld}}$ in Eq. 8). We accordingly prepared di14:

1c-BimtaPE as a probe that should show a particularly high affinity for the l_d phase, because the relative affinity of a diacyl BimtaPE for the l_o phase is markedly diminished both by decreasing its acyl chain length (compare the quenching curves for di18:0- and di14:0-BimtaPE in Fig. 4 *A*) and by increasing its degree of unsaturation (compare the quenching curves for di18:0-, 18:0/18:c-, and di18:1c-BimtaPE in Fig. 4 *A*). Interestingly, the quenching curve for di14:1c-BimtaPE in sphingomyelin/12SLPC/(33 mol% cholesterol) mixtures is essentially identical to that determined for di18:1c-BimtaPE (Fig. 4 *A*) and for a bimane-labeled conjugate (a BMS-bisPE, with the general structure shown in Fig. 1) bearing four unsaturated 18:1c acyl chains (Fig. 4 *B*). We thus conclude that these three species all exhibit negligible partitioning into l_o-phase domains in this system (save possibly in mixtures containing very high levels of sphingomyelin, which exist largely or completely in the l_o state).

Using the data analyses described in the Theory section, and assuming that di14:1c-BimtaPE exhibits negligible partitioning into the l_o phase as just discussed, we estimated the relative affinities of different diacyl BimtaPE probes for the l_o phase in sphingomyelin/12SLPC/(33 mol% cholesterol) bilayers at 37°C. These values are summarized in Table 1 as ratios $f_{lo}(X)/f_{lo}(di18:0)$, representing the estimated extent of partitioning of each fluorescent BimtaPE (X) into l_o-phase domains relative to that of the arbitrarily chosen reference species di18:0-BimtaPE. It can be seen from the results presented in Table 1 that while partitioning into the l_o phase increases with increasing chain length and decreasing unsaturation, both the shorter-chain di14:0 species and the monounsaturated 16:0/18:1c and 18:0/18:1c species still show significant partitioning into l_o domains in this system. The values presented in Table 1 were obtained by the "slope" method described in the Theory section (Eq. 8). Results obtained with this method typically gave lower standard errors but differed only modestly (by $<20\%$), and not systematically, from those obtained with the alternative "ratio" method (Eq. 7). For example, from the data shown in Fig. 2 *A*, for the species di16:0- and 18:0/18:1c-BimtaPE we determined mean values for $f_{lo}(X)/f_{lo}(di18:0)$ of 0.92 ± 0.06 and 0.38 ± 0.03, respectively, with the "slope" method and 0.78 ± 0.06 and 0.33 ± 0.15, respectively, with the "ratio" method (in the latter case averaging values estimated for samples containing 20–70% 12SLPC in the nonsterol fraction).

As noted in the Theory section, calculation of the absolute extents of partitioning of the different BimtaPEs into l_o-phase domains would require the collection of additional fluorescence data for a homologous probe that partitioned entirely into the l_o phase. To date we have not identified candidate probes that clearly fulfill this criterion. In an effort to prepare a probe that might show a higher affinity for the l_o phase than the diacyl BimtaPEs examined here, we however constructed the bimane-labeled bisPE conjugate (BMS-bisPE) shown in Fig. 1, the structure of which is essentially that of a molecule of di18:0-BimtaPE covalently linked to a second di18:0-phosphatidyl moiety. As expected, given this structural analogy, the normalized fluorescence intensities F_N measured for the tetra18:0 species in single-phase 2:1 (mol/mol) sphingomyelin/cholesterol, DPPC/cholesterol, 12SLPC/cholesterol, and TEMPO-DOPC/cholesterol vesicles were all essentially identical to those measured for di18:0-BimtaPE in the same lipid mixtures (results not shown). However, the quenching curve measured for the tetra18:0 species in the sphingomyelin/12SLPC/(33 mol% cholesterol) system at 37°C (Fig. 4 *A*) shows a markedly lower extent of quenching across the region of (l_o/l_d) phase separation than is observed for di18:0- (or di20:0-) BimtaPE. This finding indicates first that the relative affinity of even the di18:0- and di20:0-BimtaPEs for the l_o over the l_d phase in this system is still far from maximum and second, that affinity for the l_o phase can be significantly enhanced by the incorporation of additional long saturated chains into the molecule. The former conclusion agrees with the results of the detergent fractionation experiments presented later.

The exofacial leaflet of the plasma membrane in mammalian cells includes variable and, in some cases, high proportions of glycosphingolipids as well as sphingomyelin (Brown, 1998; Rietveld and Simons, 1998). In Fig. 5 *A* and Table 1 we summarize fluorescence-quenching data ob-

TABLE 1 Relative extents of partitioning of different bimane-labeled lipids into the l_o phase in phase-separated lipid mixtures

	$f_{lo}(X)/f_{lo}$ (di18:0) in					
				DPPC/TEMPO-DOPC/cholesterol		
Probe	SM/SLPC/cholesterol (37°C)	(SM+Cereb)/SLPC/cholesterol (37°C)	DPPC/12SLPC/cholesterol (25°C)	(10°C)	(25°C)	(37°C)
Di-20:0	1.21 ± 0.10	1.36 ± 0.12	1.09 ± 0.10	0.93 ± 0.11	0.75 ± 0.06	0.68 ± 0.06
Di-16:0	0.92 ± 0.06	0.58 ± 0.05	0.38 ± 0.04	0.25 ± 0.05	0.64 ± 0.04	0.76 ± 0.07
Di-14:0	0.67 ± 0.04		0.23 ± 0.02	0.048 ± 0.015	0.15 ± 0.02	0.19 ± 0.05
18:0/18:1	0.38 ± 0.03	0.15 ± 0.03	0.096 ± 0.046	0.050 ± 0.06	0.16 ± 0.01	0.14 ± 0.04
16:0/18:1	0.24 ± 0.03	0.091 ± 0.019			0.13 ± 0.01	
16:0/18:2					0.030 ± 0.007	
Tetra-18:0	2.23 ± 0.04		2.48 ± 0.39		2.47 ± 0.56	

Relative extents of partitioning of different bimane-labeled lipid probes were estimated from the data presented in Figs. 2–6, using the curve-fitting ("slope") method described in the Theory section.

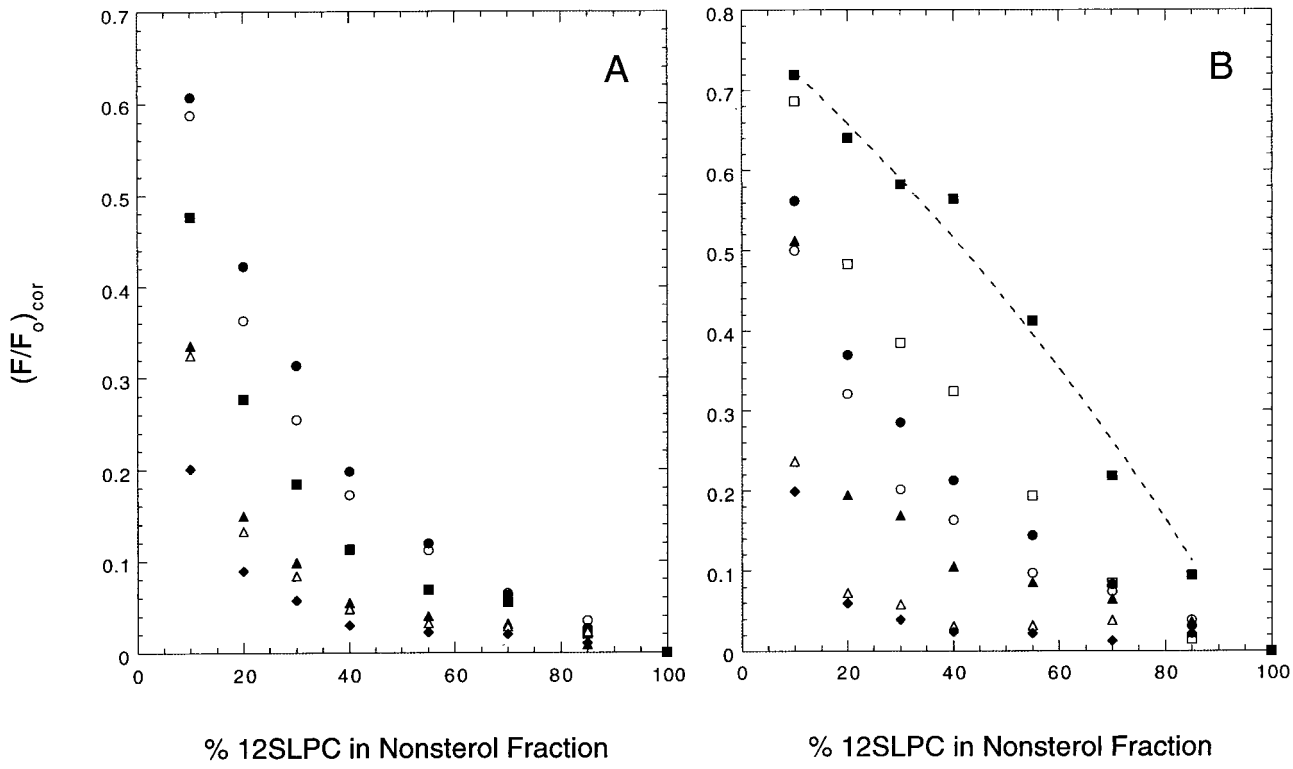

FIGURE 5 (*A*) Quenching curves obtained at 37°C for diacyl BimtaPEs in sphingolipid/12SLPC/(33 mol% cholesterol) mixtures in which 12SLPC comprised the indicated molar percentage of the nonsterol (total phospho- plus sphingolipid) fraction and a 1:1 (mol/mol) mixture of brain galactosylcerebroside and brain sphingomyelin comprised the balance of this fraction. The data shown were obtained for di20:0- (●), di18:0- (○), di16:0- (■), 18:0/18:1c- (▲), 16:0/18:1c- (△), and di14:1c-BimtaPE (◆). (*B*) Quenching curves obtained at 25°C for bimane-labeled lipids in DPPC/12SLPC/(33 mol% cholesterol) mixtures containing the indicated molar percentages of 12SLPC in the nonsterol (total phospholipid) fraction. The data shown were obtained for tetra18:0-BMS-bisPE (■) and for di18:0- (□), di16:0- (●), di14:0- (○), 18:0/18:1c- (▲), 18:1c/18:1c- (△), and di14:1c-BimtaPEs (◆). The curve shown passing through the data for tetra18:0-BMS-bisPE (*dashed line*) was obtained by fitting Eq. 1 to the data obtained for this probe in samples containing 10–85 mol% 12SLPC in the nonsterol fraction, using the values of x_Q^{ld} and $(F/F_o)_{cor}^{min}$ determined from analysis of the quenching data for all BimtaPE species as described in the text.

tained for several diacyl BimtaPEs at 37°C in sphingolipid/12SLPC/(33 mol%) cholesterol mixtures in which the sphingolipid fraction was composed of equimolar proportions of brain sphingomyelin and brain galactocerebroside. It can be seen that the relative extents of partitioning of different BimtaPEs into the l_o phase in this system vary with the acyl chain structure in a manner generally similar to that observed in the sphingomyelin/12SLPC/cholesterol mixtures discussed above. While the presence of cerebroside somewhat diminishes the relative extent of partitioning of the 16:0/18:1c- and 18:0/18:1c-BimtaPEs into l_o-phase domains compared to that of the di18:0 species, significant partitioning of the monounsaturated species into l_o domains is still observed, even in the cerebroside-containing system.

Fluorescent lipid partitioning in other (l_o/l_d) phase-separated systems

To examine the generality of the above results in other types of (l_o/l_d) phase-separated bilayers, we investigated two additional ternary systems combining two phospholipid components with cholesterol. Representative data obtained using the first of these, DPPC/12SLPC/(33 mol% cholesterol) at 25°C, are shown in Fig. 5 *B*, and the calculated relative extents of partitioning of different diacyl BimtaPEs into l_o domains in this system are presented in Table 1. As in the sphingolipid-containing systems discussed above, shorter-chain saturated and monounsaturated species show a significant ability to partition into l_o-phase domains, albeit with lesser affinity than do longer-chain saturated species. Interestingly, in this system the affinity of saturated BimtaPEs for the l_o phase does not increase monotonically with increasing acyl chain length but is essentially equal for the di18:0 and di20:0 species. However, once again the tetra18:0-BMS-bisPE conjugate (Fig. 5 *B*, *filled squares*) shows a markedly higher tendency to partition into the l_o phase than do either of these long-chain saturated species.

As a second alternative to the sphingomyelin/12SLPC/(33 mol% cholesterol) system, we also compared the (l_o/l_d) phase partitioning of different BimtaPEs in the ternary

system DPPC/TEMPO-DOPC/(33 mol% cholesterol). In this system the l_d phase-preferring lipid carries unsubstituted acyl chains and a spin-labeled polar headgroup. Fluorescence-quenching data obtained with this system for various bimane-labeled diacyl phospholipid probes are shown in Fig. 6. Control experiments (not shown) showed that different BimtaPEs gave essentially identical quenching curves in the related but homogeneous system DOPC/TEMPO-DOPC/(33 mol% cholesterol), in contrast to the markedly divergent quenching curves shown in Fig. 6. Accordingly, assuming again for this system that in a given single phase of a given composition different diacyl BimtaPEs show equal efficiencies of fluorescence quenching, we analyzed the data as described above to give the results summarized in Table 1.

In the DPPC/TEMPO-DOPC/(33 mol% cholesterol) system at 25°C, the relationship between the acyl chain structure of a BimtaPE and its relative affinity for the l_o phase is generally similar to that observed in the DPPC/12SLPC/(33 mol% cholesterol) system discussed above. The relative extent of partitioning of saturated BimtaPEs into l_o domains is greatest for the di18:0 species and decreases both for shorter and, more weakly, for longer chain lengths. Once again, however, the bimane-labeled tetra-18:0 conjugate exhibits a markedly lower extent of fluorescence quenching than does even the di18:0-BimtaPE across the region of phase separation (Fig. 6 *A*), indicating that even the latter diacyl species exhibits far from complete partitioning into l_o domains. As in the systems discussed above, the monounsaturated 16:0/18:1c and 18:0/18:1c probes show significant partitioning into the l_o phase, although the extent of this partitioning is considerably weaker than for the longer-chain disaturated species. The quenching curves for the di18:1c and di14:1c species once again are essentially superimposable, as was the quenching curve for the bimane-labeled tetra-18:1c conjugate (not shown), suggesting that these species again exhibit negligible partitioning into the l_o phase. A diunsaturated 16:0/18:2 species similarly shows a very low affinity for the l_o phase (Fig. 6 *B*).

In Fig. 6, *C* and *D*, we show fluorescence quenching curves determined for several homologous BimtaPEs in the DPPC/TEMPO-DOPC/(33 mol% cholesterol) ternary system at 37°C and at 10°C, respectively. Quantitative analysis of these quenching curves, carried out as discussed above (Table 1), indicates that at 10°C the relative extents of l_o-phase partitioning of different saturated BimtaPEs fall off much more steeply with decreasing chain length than is the case at higher temperatures. Likewise, the relative extent of partitioning of 18:0/18:1c-BimtaPE into the l_o phase vis-à-vis that of the di18:0 species is considerably smaller than at higher temperatures.

Low-temperature detergent solubilization of BimtaPEs from phase-separated bilayers

As already noted, previous estimates of the extent of partitioning of different lipid (or protein) species into l_o-phase domains in biological and artificial membranes have typically been made by measuring the fraction of such species that is resistant to solubilization by certain nonionic detergents at low temperatures. We therefore examined the relative susceptibilities of different diacyl BimtaPEs to low-temperature solubilization from (l_o/l_d) phase-separated lipid mixtures to compare these results with those of our fluorescence-based assays. To this end, large unilamellar vesicles, composed of 1:1:1 (molar proportions) DPPC/12SLPC/cholesterol or sphingomyelin/12SLPC/cholesterol and incorporating different diacyl BimtaPEs (0.6 mol%), were incubated with Triton X-100 at 0°C, then ultracentrifuged as described in Materials and Methods to separate solubilized from unsolubilized material. The proportions of each diacyl BimtaPE in the pellet and supernatant fractions were then determined, giving the results summarized in Table 2. For both lipid mixtures tested, the di18:0 probe shows the greatest and the di18:1c and di14:1c probes the smallest proportion in the unsolubilized fraction. These results are qualitatively consistent with our conclusions from the fluorescence assays discussed above. However, in both systems we also find that the percentages of the 18:0/18:1c and di14:0 species recovered in the insoluble fraction are markedly lower, compared to that of the di18:0 species (Table 2, fourth column), than we would predict based on our fluorescence-based estimates of the relative extents of partitioning of the different probes into the l_o phase in intact bilayers (last column in Table 2). These results suggest that low-temperature detergent solubilization may differentially favor excessive extraction of species that exhibit only a modest, but still significant, tendency to partition into l_o-phase domains at physiological temperatures.

(l_o/l_d) phase partitioning of prenylated peptides

Various lipidated intracellular proteins bearing two saturated acyl chains have been found to be enriched in the low-density membrane remnants isolated from mammalian cells by low-temperature detergent extraction (Arni et al., 1998; Brown and London, 1998a; van't Hof and Resh, 1997; Zlatkine et al., 1997) or by non-detergent-requiring procedures entailing sonication or alkaline extraction of membranes (Lisanti et al., 1994; Smart et al., 1995). It has been suggested that this behavior may reflect the preferential association of such proteins with liquid-ordered domains present in the cytoplasmic leaflet of the plasma membrane, which may be linked to sphingolipid-enriched domains present in the exofacial leaflet by mechanisms that remain to be elucidated (Brown and London, 1997, 1998a, 1998b; Simons and Ikonen, 1997). Prenylated proteins are less consistently found in the low-density membrane fraction isolated from cells by low-temperature detergent extraction (Chang et al., 1994; Lisanti et al., 1994; Melkonian et al., 1999). However, the identification of prenylated proteins in low-density fractions prepared from plasma

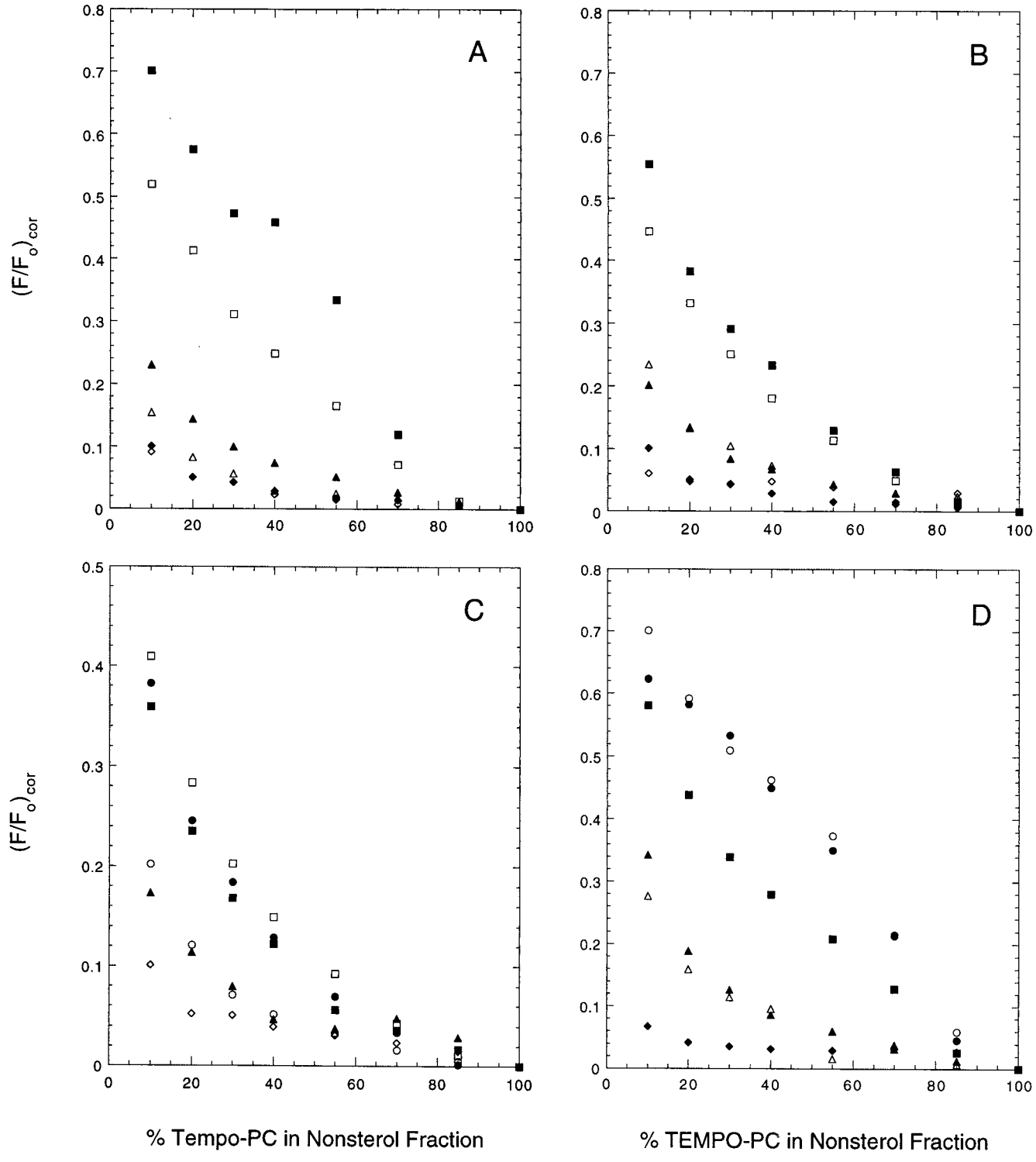

FIGURE 6 Quenching curves obtained for bimane-labeled lipids in DPPC/TEMPO-DOPC/(33 mol% cholesterol) mixtures containing the indicated molar percentages of TEMPO-DOPC in the nonsterol (total phospholipid) fraction. (*A*) Data obtained at 25°C for tetra18:0- (■) and tetra-18:1c-BMS-bisPE (◇) and for di18:0- (□), 18:0/18:1c- (▲), 16:0/18:2cc- (△), and di18:1c-BimtaPE (◆). (*B*) Data obtained at 25°C for di20:0- (■), di16:0- (□), di14:0- (△), 16:0/18:1c- (▲), di18:1c- (◆), and di14:1c-BimtaPE (◇). (*C*) Data obtained at 37°C for di20:0- (■), di18:0- (□), di16:0- (●), di14:0- (▲), 18:0/18:1c- (○), and di14:1c-BimtaPE (◇). (*D*) Data obtained at 10°C for di20:0- (○), di18:0- (●), di16:0- (■), di14:0- (▲), 18:0/18:1c- (△), and di14:1c-BimtaPE (◆).

TABLE 2 Detergent-insoluble fraction of diacyl BimtaPEs incorporated in sphingomyelin/12SLPC/cholesterol or DPPC/12SLPC/cholesterol unilamellar liposomes

Lipid composition	BimtaPE	% in pellet	(%insoluble)/(%di18:0insoluble)	$f_{lo}(X)/f_{lo}$ (di18:0)*
SphM/12SLPC/chol. (1:1:1)	di14:1c	0.30 ± 0.18		
	di18:1c	0.33 ± 0.15		
	18:0/18:1c	0.23 ± 0.10	0.019 ± 0.008*	0.38 ± 0.03
	di14:0	1.46 ± 0.10	0.111 ± 0.003*	0.67 ± 0.04
	di18:0	13.14 ± 2.14		
DPPC/12SLPC/chol. (1:1:1)	di14:1c	1.37 ± 0.45		
	di18:1c	0.72 ± 0.29		
	18:0/18:1c	1.62 ± 0.52	0.043 ± 0.014*	0.096 ± 0.046
	di14:0	4.23 ± 0.78	0.114 ± 0.011*	0.23 ± 0.02
	di18:0	37.18 ± 2.34		

Unilamellar lipid vesicles of the indicated compositions (SphM, sphingomyelin; chol., cholesterol) and incorporating 0.6 mol% of the indicated diacyl BimtaPE were incubated with 1% Triton X-100 at 0°C, and the amounts of each probe in the Triton-soluble and -insoluble fractions were measured after centrifugation as described in Materials and Methods. Values shown represent the mean (± SEM) determined for a total of six samples in three independent experiments.

*Values determined using the curve-fitting ("slope") method (Eq. 8) for the indicated BimtaPEs in sphingomyelin/12SLPC/cholesterol vesicles at 37°C or DPPC/12SLPC/cholesterol vesicles at 25°C (Table 1).

membranes by some alternative, detergent-free methods has led to suggestions that prenylated species may be highly susceptible to extraction from such fractions by detergents (Chang et al., 1994; Smart et al., 1995; Song et al., 1996). For these reasons it was of interest to evaluate directly the partitioning of prenylated peptides between liquid-ordered and liquid-disordered domains by using the present fluorescence assay. For technical reasons discussed below, these experiments were carried out using peptides bearing a dual *S*-palmitoyl/isoprenyl modification, which is found in species such as mammalian and yeast ras proteins, the yeast heterotrimeric G-protein γ-subunit Ste18p, and paralemmin (Hirschman and Jenness, 1999; Kutzleb et al., 1998; Magee et al., 1992).

Because sphingolipids generally appear to be present at relatively low levels in the cytoplasmic compared to the exofacial leaflet of the plasma membrane (Gahmberg and Hakomori, 1973; van Meer, 1989), fluorescence-quenching measurements for prenylated peptide probes were carried out using the ternary system DPPC/12SLPC/(33 mol% cholesterol). As for the fluorescent phospholipid probes discussed above, quenching curves were determined for a set of homologous lipidated peptides of the general structure shown in Fig. 1. Acceptably reproducible fluorescence data for these species (particularly the *S*-stearoyl/*S*-hexadecyl species) could be obtained only by using samples colyophilized from cyclohexane/ethanol as described in Materials and Methods. Unfortunately, even with this latter method it was not possible to obtain consistently satisfactory quenching curves for fluorescent peptides bearing single lipid chains or dual acyl modifications.

In Fig. 7 are representative quenching curves obtained for the palmitoylated/farnesylated peptide Bimta-GC(palmitoyl)GC(farnesyl)-OMe, its geranylgeranylated counterpart, and two homologous species in DPPC/12SLPC/(33 mol% cholesterol) mixtures at 25°C. It can be seen that the quenching curve for the palmitoylated/farnesylated peptide is virtually identical to that obtained for a homologous species in which the *S*-palmitoyl residue is replaced by an

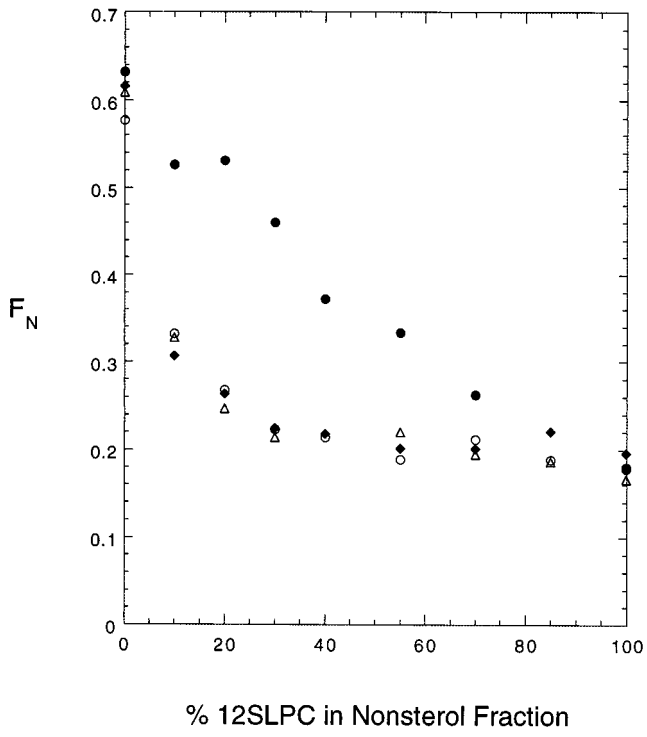

FIGURE 7 Quenching curves obtained at 25°C for bimane-labeled lipidated peptides in DPPC/12SLPC/(33 mol% cholesterol) mixtures containing the indicated molar percentages of 12SLPC in the nonsterol (total phospholipid) fraction. The data shown were obtained for Bimta-GC(16:0)GC(farnesyl)-OMe (◆), Bimta-GC(14:1c)GC(farnesyl)-OMe (○), Bimta-GC(16:0)GC(geranylgeranyl)-OMe (△), and Bimta-GC(18:0)GC(farnesyl)-OMe (●). Samples were prepared and fluorescence data were collected as described in the text.

unsaturated 14:1c-acyl residue. Because the replacement of a saturated 16:0-acyl chain by a shorter, unsaturated 14:1c-acyl residue is expected to enhance significantly the relative preference of the *S*-acylated/farnesylated peptide for the l_d phase, we can conclude that the farnesylated peptide exhibits negligible partitioning into the l_o phase regardless of whether it is modified with an unsaturated S-14:1c- or a more physiological *S*-palmitoyl chain. The quenching curve for the palmitoylated/geranylgeranylated peptide is almost identical, indicating that this species as well exhibits negligible affinity for the l_o phase. A distinctly different quenching curve is observed for the homologous lipidated peptide Bimta-GC(stearoyl)GC(hexadecyl)-OMe, which carries two long, unbranched saturated chains and which shows substantially less fluorescence quenching across the region of phase separation. This latter finding confirms that the comparatively efficient quenching of the fluorescence of the *S*-acylated/prenylated peptides within the region of phase separation is not an inherent consequence of the general structure or the site of labeling of these molecules, but instead reflects a preferential distribution of the acylated/prenylated species into the l_d phase. A similar overall pattern of results was observed for samples that were simply dried down from solvent, albeit with a significantly greater degree of scatter (not shown).

DISCUSSION

The fluorescence-quenching assay described here, which builds on the approach originally described by Feigenson and colleagues (Huang et al., 1988; London and Feigenson, 1981) to monitor the gel/liquid-crystalline partitioning of fluorescent molecules, provides a direct method for comparing the extents of partitioning of related lipids or lipidated molecules into liquid-ordered domains in systems exhibiting (l_d/l_o) phase separations. In the form described here, using bimane-labeled lipids and peptides, the assay requires that one of the major lipid components in the system be spin-labeled, to serve as an efficient quencher of probe fluorescence. However, comparison of the results obtained using chain- versus headgroup-labeled paramagnetic quenchers in this study supports the previous suggestion of London and co-workers (Ahmed et al., 1997) that in systems like those examined here the physical behavior of 12SLPC generally resembles that of an unsaturated phosphatidylcholine. Moreover, using certain types of fluorescent molecules (e.g., carbazole- or indole-labeled lipid probes; Silvius, 1992; Silvius et al., 1996), it would be possible, if desired, to replace spin-labeled lipids with brominated lipids, which can be made virtually isosteric to naturally occurring lipids, as alternative quenchers to monitor molecular partitioning between coexisting l_o and l_d phases.

Our measurements of the relative abilities of different bimane-labeled diacyl phospholipids to partition into l_o domains generally support previous conclusions, based on detergent extraction assays (Schroeder et al., 1994), that longer-chain disaturated species are relatively enriched in such domains while multiply unsaturated species show very little partitioning into the l_o phase. Our findings thus lend further support to previous suggestions that glycosyl-phosphatidylinositol (GPI)-anchored proteins of the cell surface may associate with l_o-phase "lipid rafts" at least in part because their lipid anchors frequently carry two long saturated acyl chains (Benting et al., 1999; McConville and Ferguson, 1993; Schroeder et al., 1994). However, our present results add to this conclusion the nuance that monounsaturated species, or species bearing saturated chains as short as C_{14} (myristoyl), may also be able to partition to a significant degree into l_o domains under physiological conditions, albeit with significantly lower affinities than do longer-chain disaturated lipids. From this perspective it is particularly interesting to note that shorter-chain (di14:0-) or monounsaturated (18:0/18:1c-) BimtaPEs show much weaker partitioning (relative to their long-chain saturated counterparts) into the low-temperature detergent-insoluble fraction isolated from mixed-phase (l_o/l_d) bilayers than they do into l_o-domains in intact bilayers of the same compositions (Table 2). These results indicate that the finding that a particular species is depleted from membrane remnants obtained by low-temperature detergent extraction may not preclude the possibility that a significant fraction of that species could partition into l_o-phase domains in the intact membrane.

A possible explanation for the discrepancy just noted between the conclusions of the detergent extraction and the fluorescence-quenching assays is suggested by our observations of the effects of temperature on the relative extents of partitioning of different diacyl phospholipid probes into l_o-phase domains (Table 1). At 10°C in DPPC/TEMPO-DOPC/cholesterol bilayers, partitioning of di14:0- and 18:0/18:1c-BimtaPE into l_o domains relative to that of di18:0-BimtaPE is seen to decline markedly (by three- to fourfold) compared to the levels of partitioning of these same probes (again assessed relative to that of the di18:0 species) at 25°C or 37°C (Table 1). Thus it is plausible to suggest that the low temperatures (0–4°C) normally used to isolate detergent-resistant membrane domains may promote significant enrichment of long-chain disaturated species in these domains relative to other species (e.g., diacylated molecules bearing monounsaturated or shorter saturated lipid chains) that exhibit less pronounced but potentially still significant partitioning into such domains at physiological temperatures.

Although, as already noted, the extent of partitioning of saturated lipids into l_o-phase domains is generally greater for longer-chain species, our results indicate that in DPPC-containing ternary lipid mixtures, partitioning into this phase is maximum for the di18:0-BimtaPE and is either comparable or significantly lower for the di20:0 homolog. It

thus appears that the relative affinity of a lipid or lipid-anchored molecule for the l_o versus the l_d phase is determined by factors more complex than the molecule's chain-melting temperature alone (e.g., by optimal versus suboptimal matching of the chain length of the molecule to the thickness of the l_o domains). Similar conclusions have been reported previously for the partitioning of an unrelated series of homologous fluorescent molecules between gel and liquid-crystalline phases in sterol-free lipid bilayers (Spink et al., 1990).

Our observation that lipid conjugates (BMS-bisPEs) bearing four long saturated acyl chains show markedly greater partitioning into l_o-phase domains than do analogous diacyl species suggests that the oligomerization (e.g., by cross-linking) of lipids or lipid-anchored molecules bearing saturated acyl chains may enhance their relative affinities for l_o-phase domains. As discussed previously (Brown and London, 1998a), this phenomenon could in principle play a significant role in the reported redistribution of species such as glycosphingolipids and glycosylphosphatidylinositol-anchored proteins to particular subdomains of the plasma membrane upon cross-linking (Fujimoto, 1996; Harder et al., 1998; Mayor et al., 1994). The observed 2.2–2.5-fold greater affinity of the tetra- versus di-18:0 lipid probes examined here for the l_o over the l_d phase may appear rather modest. However, if we assume that each saturated diacyl moiety contributes in an additive manner to the overall free energy of l_o/l_d phase partitioning, we can readily calculate, for example, that even a tetrameric complex of a di-18:0 species would exhibit a 10–15-fold greater affinity for the l_o phase than would the monomer, which could support a very substantial redistribution of the oligomerized species within a mixed-phase (l_o/l_d) membrane bilayer.

Our measurements of the distributions of different lipidated peptides between coexisting l_d and l_o phases support previous suggestions that prenylated molecules, by virtue of their branched and multiply unsaturated hydrocarbon chains, show a negligible tendency to partition into liquid-ordered domains (Melkonian et al., 1999). Peptides bearing a dual *S*-palmitoyl/*S*-isoprenyl modification, a motif found at the carboxyl termini of proteins such as mammalian H- and N-ras and yeast Ste18p (Hirschman and Jenness, 1999; Magee et al., 1992), showed a negligible ability to partition into the l_o phase in the DPPC/12SLPC/cholesterol system examined here. Because the saturated *S*-palmitoyl chains of these peptides would themselves be expected to favor partitioning into l_o-phase domains, we can infer that the cysteine-coupled prenyl group itself shows a strong preference for association with the l_d over the l_o phase. Unfortunately, as already noted, for technical reasons this conclusion could not be tested directly with the present assay system. However, in agreement with this prediction, using direct measurements of lipid/water partition coefficients (Silvius and l'Heureux, 1994), we have found that prenylated peptides partition at least 10-fold more weakly into l_o-phase than into l_d-phase lipid vesicles at physiological temperatures (Wang and Silvius, unpublished results). Our present findings thus agree very well with the recent conclusion of Moffett et al. (2000), based on the results of low-temperature detergent-extraction experiments, that the prenylated γ-subunits of heterotrimeric G-proteins are excluded from lipid rafts both as $\beta\gamma$ dimers and when additionally complexed to myristoylated/*S*-palmitoylated $G\alpha_i$-subunits. Our results thus suggest that the recruitment of prenylated proteins to "lipid raft" structures in mammalian cell membranes, even when such proteins are additionally mono-*S*-acylated, will require some favorable protein-protein interaction (Song et al., 1996) to overcome the tendency of the prenyl moiety to be excluded from l_o-phase domains.

It remains an open question whether the conclusion just noted would apply as well to proteins that can be multiply *S*-palmitoylated as well as prenylated, as is possible, for example, for H-ras and paralemmin (Kutzleb et al., 1998; Magee et al., 1992), and, if not, whether multiple *S*-acylation of such proteins might serve physiologically to modulate the affinity of their lipidated "anchor" sequences for l_o-phase domains. We are currently investigating possible experimental approaches to allow additional classes of lipidated peptides (and other species) to be examined in the present fluorescence assay so that such further questions of this nature can be addressed.

This research was supported by an operating grant from the Medical Research Council of Canada (MT-7776) to JRS and by a Studentship Award from the Natural Science and Engineering Research Council of Canada to T-YW.

REFERENCES

Ahmed, S. N., D. A. Brown, and E. London. 1997. On the origin of sphingolipid/cholesterol-rich detergent-insoluble cell membranes: physiological concentrations of cholesterol and sphingolipid induce formation of a detergent-insoluble, liquid-ordered phase in model membranes. *Biochemistry.* 36:10944–10953.

Arni, S., S. A. Keilbaugh, A. G. Ostermeyer, and D. A. Brown. 1998. Association of GAP-43 with detergent-resistant membranes requires two palmitoylated cysteine residues. *J. Biol. Chem.* 273:28478–28485.

Barrantes, J. R. 1998. Applied Mathematics for Physical Chemistry, 2nd Ed. Prentice-Hall, Upper Saddle River, NJ.

Benting, J., A. Rietveld, I. Ansorge, and K. Simons. 1999. Acyl and alkyl chain length of GPI-anchors is critical for raft association in vitro. *FEBS Lett.* 462:47–50.

Brown, D. A., and E. London. 1997. Structure of detergent-resistant membrane domains: does phase separation occur in biological membranes? *Biochem. Biophys. Res. Commun.* 240:1–7.

Brown, D. A., and E. London. 1998a. Structure and origin of ordered lipid domains in biological membranes. *J. Membr. Biol.* 164:103–114.

Brown, D. A., and E. London. 1998b. Functions of lipid rafts in biological membranes. *Annu. Rev. Cell Dev. Biol.* 14:111–136.

Brown, D. A., and J. K. Rose. 1992. Sorting of GPI-anchored proteins to glycolipid-enriched membrane subdomains during transport to the apical cell surface. *Cell.* 68:533–544.

Brown, R. E. 1998. Sphingolipid organization in biomembranes: what physical studies of model membranes reveal. *J. Cell Sci.* 111:1–9.

Chang, W. J., Y. S. Ying, K. G. Rothberg, N. M. Hooper, A. J. Turner, H. A. Gambliel, J. De Gunzburg, S. M. Mumby, A. G. Gilman, and R. G. Anderson. 1994. Purification and characterization of smooth muscle cell caveolae. *J. Cell Biol.* 126:127–138.

Chattopadhyay, A., and E. London. 1987. Parallax method for direct measurement of membrane penetration depth utilizing fluorescence quenching by spin-labeled phospholipids. *Biochemistry.* 26:39–45.

Cinek, T., and V. A. Horejsí. 1992. The nature of large noncovalent complexes containing glycosyl-phosphatidylinositol-anchored membrane glycoproteins and protein tyrosine kinases. *J. Immunol.* 149: 2262–2270.

Fujimoto, T. 1996. GPI-anchored proteins, glycosphingolipids, and sphingomyelin are sequestered to caveolae only after cross-linking. *J. Histochem. Cytochem.* 44:929–941.

Gaffney, B. J. 1976. The chemistry of spin labels. *In* Spin Labeling: Theory and Applications. L. J. Berliner, editor. Academic Press, New York. 184–238.

Gahmberg, C. T., and S. I. Hakomori. 1973. External labeling of cell surface galactose and galactosamine in glycolipid and glycoprotein of human erythrocytes. *J. Biol. Chem.* 248:4311–4317.

Harder, T., P. Scheiffele, P. Verkade, and K. Simons. 1998. Lipid domain structure of the plasma membrane revealed by patching of membrane components. *J. Cell Biol.* 141:929–942.

Hirschman, J. E., and D. D. Jenness. 1999. Dual lipid modification of the yeast gamma subunit Ste18p determines membrane localization of $G_{\beta\gamma}$. *Mol. Cell Biol.* 19:7705–7711.

Huang, N., K. I. Florine-Castel, G. W. Feigenson, and C. H. Spink. 1988. Effect of fluorophore linkage position of *n*-(9-anthroyloxy) fatty acids on probe distribution between coexisting gel and fluid phospholipid phases. *Biochim. Biophys. Acta.* 939:124–130.

Kutzleb, C., G. Sanders, R. Yamamoto, X. Wang, B. Lichte, E. Petrasch-Parwez, and M. W. Kilimann. 1998. Paralemmin, a prenyl-palmitoyl-anchored phosphoprotein abundant in neurons and implicated in plasma membrane dynamics and cell process formation. *J. Cell Biol.* 143: 795–813.

Lisanti, M. P., P. E. Scherer, J. Vidugiriene, Z. Tang, A. Hermanowski-Vosatka, Y. H. Tu, R. F. Cook, and M. Sargiacomo. 1994. Characterization of caveolin-rich membrane domains isolated from an endothelial-rich source: implications for human disease. *J. Cell Biol.* 126:111–126.

London, E., and G. W. Feigenson. 1981. Fluorescence quenching in model membranes. 1. Characterization of quenching caused by a spin-labeled phospholipid. *Biochim. Biophys. Acta.* 649:89–97.

MacDonald, R. C., R. I. MacDonald, B. P. Menco, K. Takeshita, N. K. Subbarao, and L. R. Hu. 1991. Small-volume extrusion apparatus for preparation of large, unilamellar vesicles. *Biochim. Biophys. Acta.* 1061: 297–303.

Magee, A. I., C. M. Newman, T. Giannakouros, J. F. Hancock, E. Fawell, and J. Armstrong. 1992. Lipid modifications and function of the ras superfamily of proteins. *Biochem. Soc. Trans.* 20:497–499.

Mayor, S., K. G. Rothberg, and F. Maxfield. 1994. Sequestration of GPI-anchored proteins in caveolae triggered by cross-linking. *Science.* 264:1948–1951.

McConville, M. J., and M. A. J. Ferguson. 1993. The structure, biosynthesis and function of glycosylated phosphatidylinositols in the parasitic protozoa and higher eukaryotes. *Biochem. J.* 294:305–324.

Melkonian, K. A., A. G. Ostermeyer, J. Z. Chen, M. G. Roth, and D. A. Brown. 1999. Role of lipid modifications in targeting proteins to detergent-resistant membrane rafts. Many raft proteins are acylated, while few are prenylated. *J. Biol. Chem.* 274:3910–3917.

Moffett, S., D. A. Brown, and M. E. Linder. 2000. Lipid-dependent targeting of G proteins into rafts. *J. Biol. Chem.* 275:2191–2198.

Rietveld, A., and K. Simons. 1998. The differential miscibility of lipids as the basis for the formation of functional membrane rafts. *Biochim. Biophys. Acta.* 1376:467–479.

Rodgers, W., B. Crise, and J. K. Rose. 1994. Signals determining protein tyrosine kinase and glycosyl-phosphatidylinositol-anchored protein targeting to a glycolipid-enriched membrane fraction. *Mol. Cell. Biol.* 14:5384–5391.

Sargiacomo, M., M. Sudol, Z. Tang, and M. P. Lisanti. 1993. Signal transducing molecules and glycosyl-phosphatidylinositol-linked proteins form a caveolin-rich insoluble complex in MDCK cells. *J. Cell Biol.* 122:789–808.

Schroeder, H., R. Leventis, S. Rex, M. Schelhaas, E. Nägele, H. Waldmann, and J. R. Silvius. 1997. S-Acylation and plasma membrane targeting of the farnesylated carboxyl-terminal peptide of N-ras in mammalian fibroblasts. *Biochemistry.* 36:13102–13109.

Schroeder, R. J., S. N. Ahmed, Y. Zhu, E. London, and D. A. Brown. 1998. Cholesterol and sphingolipid enhance the Triton X-100 insolubility of glycosylphosphatidylinositol-anchored proteins by promoting the formation of detergent-insoluble ordered membrane domains. *J. Biol. Chem.* 273:1150–1157.

Schroeder, R., E. London, and D. Brown. 1994. Interactions between saturated acyl chains confer detergent resistance on lipids and glycosylphosphatidylinositol (GPI-) anchored proteins: GPI-anchored proteins in liposomes and cells show similar behavior. *Proc. Natl. Acad. Sci. USA.* 91:12130–12134.

Shahinian, S., and J. R. Silvius. 1995. Doubly-lipid-modified protein sequence motifs exhibit long-lived anchorage to lipid bilayer membranes. *Biochemistry.* 34:3813–3822.

Shenoy-Scaria, A. M., L. K. Gauen, J. Kwong, A. S. Shaw, and D. M. Lublin. 1993. Palmitylation of an amino-terminal cysteine motif of protein tyrosine kinases $p56^{lck}$ and $p59^{fyn}$ mediates interaction with glycosylphosphatidylinositol-anchored proteins. *Mol. Cell. Biol.* 13: 6385–6392.

Shenoy-Scaria, A. M., J. Kwong, T. Fujita, M. W. Olszowy, A. S. Shaw, and D. M. Lublin. 1992. Signal transduction through decay-accelerating factor. Interaction of glycosyl-phosphatidylinositol anchor and protein tyrosine kinases $p56^{lck}$ and $p59^{fyn}$. *J. Immunol.* 149:3535–3541.

Silvius, J. R. 1992. Cholesterol modulation of lipid intermixing in phospholipid and glycosphingolipid mixtures. Evaluation using fluorescent lipid probes and brominated lipid quenchers. *Biochemistry.* 31: 3398–3408.

Silvius, J. R., D. del Giudice, and M. Lafleur. 1996. Cholesterol at different bilayer concentrations can promote or antagonize lateral segregation of phospholipids of differing acyl chain length. *Biochemistry.* 35: 15198–15208.

Silvius, J. R., and R. Leventis. 1993. Spontaneous interbilayer transfer of phospholipids: dependence on acyl chain composition. *Biochemistry.* 32:13318–13326.

Silvius, J. R., and F. l'Heureux. 1994. Fluorimetric evaluation of the affinities of isoprenylated peptides for lipid bilayers. *Biochemistry.* 33:3014–3022.

Silvius, J. R., and M. J. Zuckermann. 1993. Interbilayer transfer of phospholipid-anchored macromolecules via monomer diffusion. *Biochemistry.* 32:3153–3161.

Simons, K., and E. Ikonen. 1997. Functional rafts in cell membranes. *Nature.* 387:569–572.

Smart, E. J., Y. S. Ying, C. Mineo, and R. G. Anderson. 1995. A detergent-free method for purifying caveolae membrane from tissue culture cells. *Proc. Natl. Acad. Sci. USA.* 92:10104–10108.

Song, S. K., S. Li, T. Okamoto, L. A. Quilliam, M. Sargiacomo, and M. P. Lisanti. 1996. Co-purification and direct interaction of Ras with caveolin, an integral membrane protein of caveolae microdomains. Detergent-free purification of caveolae microdomains. *J. Biol. Chem.* 126: 9690–9697.

Spink, C. H., M. D. Yeager, and G. W. Feigenson. 1990. Partitioning behavior of indocarbocyanine probes between coexisting gel and fluid phases in model membranes. *Biochim. Biophys. Acta.* 1023:25–33.

van Meer, G. 1989. Lipid traffic in animal cells. *Annu. Rev. Cell Biol.* 5:247–275.

van't Hof, W., and M. D. Resh. 1997. Rapid plasma membrane anchoring of newly synthesized $p59^{fyn}$: selective requirement for NH_2-terminal myristoylation and palmitoylation at cysteine-3. *J. Cell Biol.* 136: 1023–1035.

Zlatkine, P., B. Mehul, and A. I. Magee. 1997. Retargeting of cytosolic proteins to the plasma membrane by the Lck protein tyrosine kinase dual acylation motif. *J. Cell Sci.* 110:673–679.